



Multi-Objective Optimization of Nano-Silica Modified Cement-Based Materials Mixed With Supplementary Cementitious Materials Based on Response Surface Method

Xiuzhi Zhang^{1,2*}, Liming Lin^{1,2}, Mengdi Bi³, Hailong Sun^{1,2}, Heng Chen^{1,2}, Qinfei Li^{1,2} and Ru Mu³

¹School of Materials Science and Engineering, University of Jinan, Jinan, China, ²Shandong Provincial Key Laboratory of Preparation and Measurement of Building Materials, University of Jinan, Jinan, China, ³School of Civil and Transportation Engineering, Hebei University of Technology, Tianjin, China

OPEN ACCESS

Edited by:

Kequan Yu,
Tongji University, China

Reviewed by:

Jian Huang,
Wuhan University of Technology,
China
Yun Gao,
Southeast University, China

*Correspondence:

Xiuzhi Zhang
mse_zhangxz@ujn.edu.cn

Specialty section:

This article was submitted to
Structural Materials,
a section of the journal
Frontiers in Materials

Received: 20 May 2021

Accepted: 30 August 2021

Published: 07 October 2021

Citation:

Zhang X, Lin L, Bi M, Sun H, Chen H,
Li Q and Mu R (2021) Multi-Objective
Optimization of Nano-Silica Modified
Cement-Based Materials Mixed With
Supplementary Cementitious Materials
Based on Response Surface Method.
Front. Mater. 8:712551.
doi: 10.3389/fmats.2021.712551

This paper investigates the effect of supplementary cementitious materials (SCMs) on the fresh and mechanical properties of nano-silica modified cement-based materials (NSMCBM) based on the response surface method (RSM). Fly ash (FA), ground granulated blast-furnace slag (GGBFS), and silica fume (SF) were selected and the Box-Behnken design (BBD) method was used to design mix proportion. Besides, the quadratic term model was used to describe the relationship between independent variables and responses including fluidity, yield stress, plastic viscosity, thixotropy, and 3, 7, 28, and 56 d compressive strength. Based on the quadratic term model, the response surface of each response was drawn to understand the influence of SCMs. Results showed that FA had significant effect on fluidity and thixotropy while three kinds of SCMs had extremely significant effect on plastic viscosity. Response surface plot showed that NS could increase the plastic viscosity of NSMCBM to 1.445 Pa•s (M16). However, the addition of FA and GGBFS decreased the plastic viscosity to 0.9 Pa•s, which was comparable with the reference sample (M17). Such value was 37.7% lower than that of M16. Meanwhile, NS complemented the reduction of compressive strength caused by SCMs. Thus, the synergy effect of SCMs and NS could improve both fresh and mechanical properties. At last, multi-objective optimization was utilized to optimize the proportion of SCMs considering the interaction between SCMs to achieve desirable parameters.

Keywords: response surface method (RSM), multi-objective optimization, nano-silica, supplementary cementitious materials (SCM), rheology

INTRODUCTION

With the development of concrete technology, supplementary cementitious materials (SCMs) have grown up to be indispensable components in concrete. It not only reduces cost but also improves the workability and durability of concrete (Cheng et al., 2018; Dhanya et al., 2018). However, the incorporation of SCMs decreases the early strength significantly, especially with the incorporation of large amounts of SCMs such as in pumped concrete and self-compacting concrete (SCC). Even

though adding accelerators such as calcium chloride (Riding et al., 2010), triethanolamine (Yan-Rong et al., 2016), and nitrate (Pizoń et al., 2016) can compensate for the adverse effects caused by the large amount of SCMs, but the improvement of early strength is limited and some accelerators also lead to the reduction of long term mechanical properties of concrete (Pizoń, 2017).

Due to its higher pozzolanic reactivity and nucleation effect (García-Taengua et al., 2015; Flores et al., 2017), nano-silica (NS) is regarded as a promising modifying material for concrete, which can improve the mechanical strength and durability of the cement-based materials and thus complement the reduction of early strength caused by SCMs. However, the consequent disadvantage is that the NS has a large specific surface area, so the rheological properties have deteriorated when it is incorporated into the cement paste (Ghafari et al., 2014). It is worth noting that a large number of literatures have reported that SCMs can improve the workability of nano-silica modified cement-based materials (NSMCBM) owing to the “morphological effect” and “filling effect” (Jalal et al., 2019; Roshani and Fall 2020; Hosan and Shaikh, 2021). Thus, the combination of NS and SCMs can improve various aspects of properties (workability, rheology, and mechanical properties) and has achieved satisfying results (Flores et al., 2017; Nandhini and Ponmalar, 2018; Ramezani pour and Moeini, 2018; Liu et al., 2019). However, the optimum dosage of SCMs lacks a theoretical basis to achieve desirable properties. Besides, the interaction effect between SCMs also makes the properties of NSMCBM complicated and hard to predict. For this reason, it is important to investigate the influence of SCMs on workability and mechanical properties of NSMCBM. At the same time, the proportion of SCMs should be optimized to obtain satisfying properties.

The most widely used method for optimizing parameters is the response surface method (RSM). RSM is a statistical method to solve multivariate problems, which includes central composite design (CCD) method and Box-Behnken design (BBD) method (Pratama et al., 2020). Compared with the control variates method, RSM has less workload and more scientific experimental design (Ghalehnavi et al., 2020). As an effective statistical method, the RSM method has been widely employed in civil engineering to optimize the properties of concrete. For the CCD method, Jiao et al. (2018) optimized the mixture design of concrete based on the rheological properties. Li et al. (2018) optimized the mix proportion to prepare high-performance alkali-activated concrete with a slump of more than 200 mm. For the BBD method, Ahmed et al. (2020) employed the BBD method to get the optimum solution for designing parameters, which attained maximum mechanical properties and recycled aggregate, as well as minimum fiber percentage. However, few literatures can be found about the SCMs optimization due to their complex compositions, especially the incorporation of NS, which should be further researched to explore the synergy effect between SCMs and NS.

In this paper, three kinds of SCMs, namely, fly ash (FA), ground granulated blast-furnace slag (GGBFS), and silica fume (SF), were selected to explore the effect of the types, dosage, and interaction on the fluidity, rheology, and compressive strength of nano-silica modified cement-based materials (NSMCBM) based on RSM. Among them, the Box-Behnken design (BBD) method was used

to design the mix proportion. Analysis of variance (ANOVA) was utilized to describe the significance of the factors and the fitting equation was determined according to the experimental results, and then, the combined effect of SCMs on fluidity, rheology, and compressive strength of NSMCBM was analyzed. Finally, the proportion of SCMs was optimized according to the fitting equation to achieve desirable properties. The authors hoped this study can provide an approach for optimizing mix proportion, especially multi-blending SCMs.

MATERIALS AND METHODS

Materials

The cement used here was Portland cement (P.O 42.5), which complies with Chinese standard GB 175-2007 (Committee, 2016). FA, GGBFS, and SF, these three kinds of supplementary cementitious materials (SCMs) were selected. The chemical compositions of cement and SCMs are shown in **Table 1**. The characteristic particle size measured by laser particle size analyzer and specific surface area measured by BET are given in **Table 2**. The microscopic morphology photographed by scanning electron microscope (SEM) is presented in **Figures 1–4**. There are many kinds of nano-silica (NS) and the pyrogenic fumed nano-silicas were used in this study. The nano-silica with 99.8% of powder concentration was used and its particle size is 7–40 nm. The characteristic particle size and specific surface area are presented in **Table 2**. A polycarboxylate-based superplasticizer (SP) with a water-reducing rate of 40% was used and its solid content is 45%.

Mix Proportion and Sample Preparation

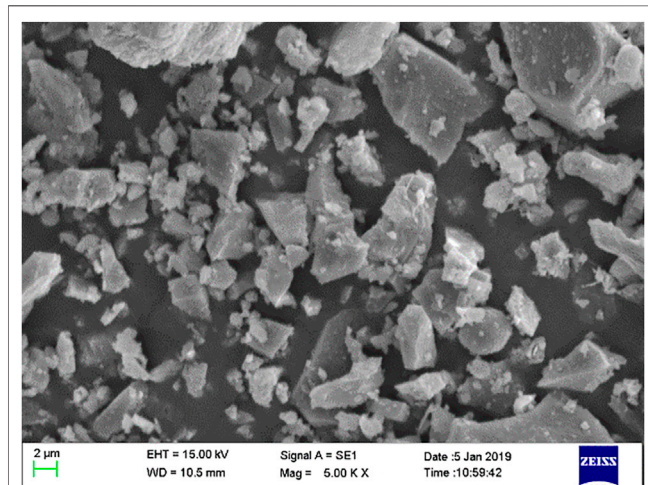
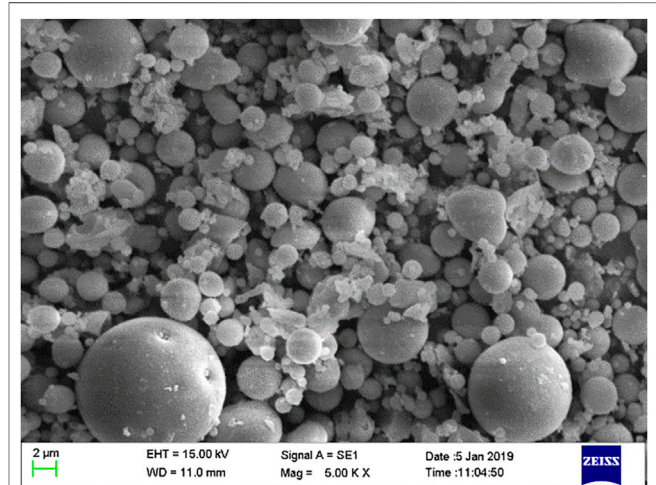
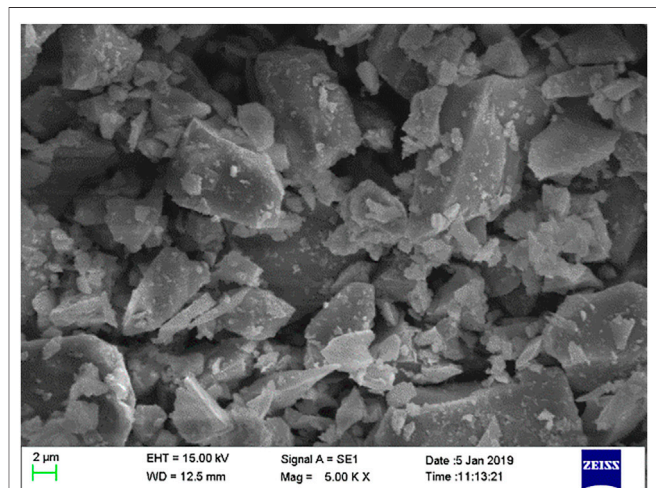
In this study, the effect of SCMs was only focused on. Therefore, the effect of fine and coarse aggregate was neglected and the nano-silica modified cement-based paste was prepared in which the amount of SP was 0.5% by mass of binder, and the water-to-binder ratio was 0.3. NS was determined as 1% by mass of binder because Ref. (Hou et al., 2012; Hou et al., 2013) showed that NS would be difficult to disperse when the amount of NS is larger than 1.2%, even if ultrasonic dispersion is used. Besides, FA, GGBFS, and SF were used to replace cement for preparing ternary (cement, NS, and any one of the three SCMs), quaternary (cement, NS, and any two of the three SCMs), and quinary (cement, NS, and three SCMs) paste. The replacement levels for various SCMs were differed as 0, 15, and 30% for FA and GGBFS and 0, 3, and 6% for SF. Each of the SCMs was replaced by a percentage of the mass of the cement. According to the Box-Behnken design (BBD) method, fifteen groups of mix proportion were required and the corresponding lowest, median, and maximum values of replacement levels of SCMs were coded by -1 , 0 , and $+1$, respectively. Besides, to understand the effect of NS on workability and mechanical strength, two groups of paste that only contained cement and only contained cement and NS were prepared. The schematic of BBD is shown in **Figure 5** and the detailed mix proportion can be found in **Table 3**. It should be noted that for convenience, each group was marked by letter plus number, where F stood for fly ash, G stood for ground

TABLE 1 | Chemical composition of cement and SCMs.

	CaO	SiO ₂	Al ₂ O ₃	MgO	Fe ₂ O ₃	SO ₃	Na ₂ O	TiO ₂	K ₂ O	Others
Cement	59.5	19.18	4.93	3.95	3.10	3.47	0.21	—	0.32	5.34
FA	3.79	47.20	41.29	1.10	2.51	1.17	0.91	0.69	—	1.34
GGBFS	39.8	35.4	12.8	7.9	0.2	1.9	0.3	—	0.4	1.3
SF	0.43	97.20	0.08	0.27	—	0.57	0.46	—	0.83	0.16

TABLE 2 | Characteristic particle size and specific surface area of cement, SCMs, and NS.

	D ₁₀ /μm	D ₅₀ /μm	D ₉₀ /μm	Mean/μm	Specific surface area/(m ² /kg)
Cement	1.29	13.24	35.57	16.54	328
FA	0.61	6.27	22.64	8.62	640
GGBFS	1.26	8.38	24.85	10.66	594
SF	0.056	0.14	0.21	0.15	20,000
NS	0.0065	0.023	0.04	0.029	2,96,000

**FIGURE 1** | SEM images of cement and SCMs, cement.**FIGURE 2** | SEM images of cement and SCMs, fly ash.**FIGURE 3** | SEM images of cement and SCMs, ground granulated blast-furnace slag.

granulated blast-furnace slag, and S stood for silica fume. The number after the letter represented the corresponding amounts.

NS is easy to agglomerate due to its ultra-fine particle size when mixed with water (Kong et al., 2012). Therefore, high-intensity ultrasonication (SB25-12 DTD, 600 W, 40 Hz) was used to disperse suspension. Different mixing orders of raw materials will lead to significant deviation or uncertainty of the experimental results (Wang et al., 2019). In order to improve the accuracy of the results and reduce the deviation, each group of mixture was prepared according to the following mixing protocol. Firstly, the nano-silica suspension, water, and superplasticizer were mixed and poured into the mixing container to mix with cement and/or supplementary cementitious materials. Secondly, it was mixed at a lower speed of 150 r/min for 2 minutes and then at a higher speed of 300 r/min for additional 2 minutes to get evenly paste (Xiuzhi et al., 2021). After finishing the preparation, the measurement of fluidity and rheological parameters was carried out.

Testing Methods

Fluidity

According to the American standard ASTM C230 (ASTM International, 2014), the fluidity was measured with a mini cone whose top diameter was 36 mm, the bottom diameter was 60 mm, and the height was 60 mm. At first, the mini cone was laid on a wet horizontal glass board and filled with paste and

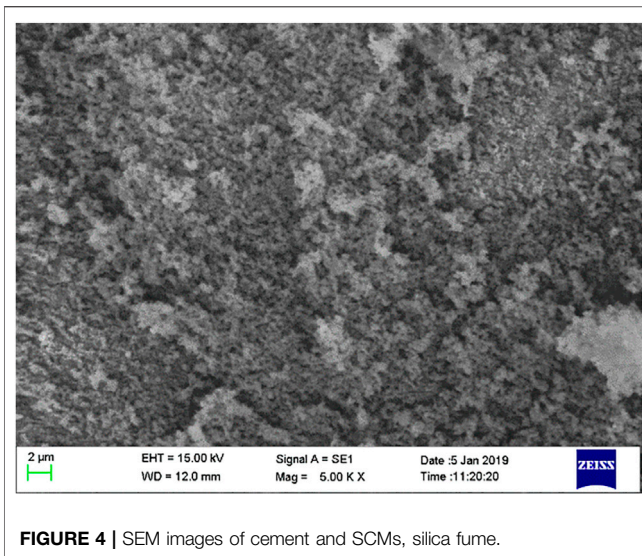


FIGURE 4 | SEM images of cement and SCMs, silica fume.

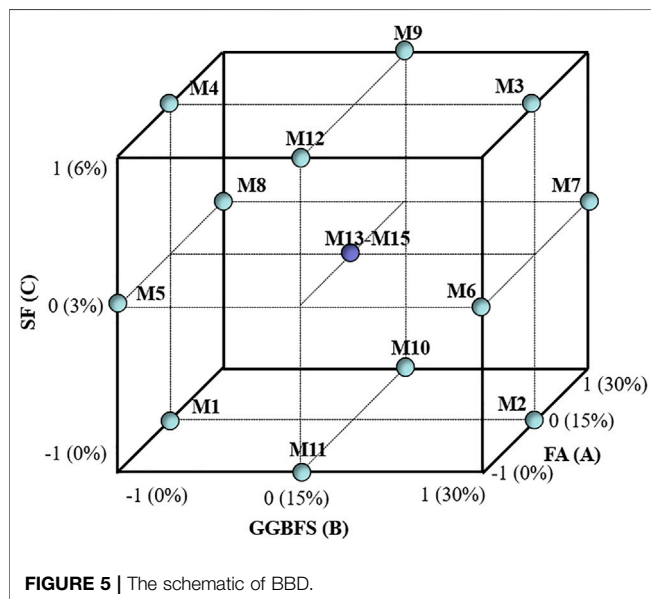


FIGURE 5 | The schematic of BBD.

then the mini cone was lifted. After waiting for 30 s, two diameters perpendicular to each other of each paste were measured and the average value was recorded as fluidity.

Rheological Parameters

The rheological parameters were determined by a Malvern Kinexus rotary rheometer. The measurement procedures were as follows: the sample was pre-sheared for 30 s at a shear rate of 100 s^{-1} . After resting for 30 s, the shear rate increased from 0 to 150 s^{-1} uniformly in 120 s and finally dropped to 0 s^{-1} with the same rotation speed gradient. The detailed process can be seen in Figure 6. This measurement procedure can minimize the internal flocculation structure of the paste before testing the rheological parameters, making the test results more accurate (Park et al., 2005; Senff et al., 2009).

According to the data measured by the rheometer, the descending section was selected to draw the shear stress-shear rate curve and the Herschel-Bulkley model was used to fit the rheological curve:

$$\tau = \tau_0 + K\dot{\gamma}^n, \quad (1)$$

where τ and $\dot{\gamma}$ are shear stress and shear rate, respectively; τ_0 is yield stress; K is the consistency coefficient; n is the power exponent.

The plastic viscosity η was calculated according to the method proposed by de Larrard (Hu and de Larrard, 1996; de Larrard et al., 1998). The equation is as follows:

$$\eta = \frac{3K}{n+2}\dot{\gamma}_{max}^{n-1}. \quad (2)$$

Several methods have been utilized to measure the thixotropy (Qian et al., 2018): shear rate decay method (Kawashima et al., 2013), yield stress growth rate (Roussel, 2006), and thixotropy hysteresis loop (Ferron et al., 2007). In this study, the thixotropy hysteresis loop was applied. According to the data measured by the rheometer, the thixotropic hysteresis loops can be obtained and the area of loops can be used to characterize the thixotropy.

Compressive Strength

After the fresh properties were measured, the paste was cast into $20 \times 20 \times 20 \text{ mm}^3$ molds and covered by a plastic film. After 1 day, the species were demolded and put into a standard curing room at $20 \pm 2^\circ\text{C}$ and relative humidity higher than 95% to cure for 3, 7, 28, and 56 days. Finally, CMT-5504 electronic universal testing machine was used to measure the compressive strength. The displacement velocity was 2.0 mm/min . The compressive strength of species was measured according to Chinese standard GB/T 17671-1999 (Supervision, 1999) and the average value of three species of each group was recorded as the final compressive strength.

Analyzing Methods

In most RSM problems, the relationship between the response (dependent variable) and the independent variable is unknown, so the first step of RSM is to seek a suitable approximation of the true functional relationship between the response (y) and the independent variable (x). Generally speaking, if the response is suitable for modeling with a linear function of independent variables, the approximate function is a linear model:

$$y = \beta_0 + \beta_1 x_1 + \beta_2 x_2 + \dots + \beta_k x_k + \varepsilon. \quad (3)$$

Otherwise, higher-order polynomials must be used. For example, the expression of the quadratic term model is

$$y = \beta_0 + \sum_{i=1}^k \beta_i x_i + \sum_{i=1}^k \beta_{ii} x_i^2 + \sum_{i=1}^k \sum_{j>1}^k \beta_{ij} x_i x_j + \varepsilon, \quad (4)$$

where y is the response variable; x_i , x_i^2 , $x_i x_j$ are the independent variables; k is the number of independent variables; β represents the regression coefficients; ε is the random error. In this study, the quadratic term model was used to fit the data to obtain the

TABLE 3 | Mix proportion of nano-silica modified cement-based paste containing SCMs.

Groups	Coded values			Cementitious mass/%				
	FA (A)	GGBFS (B)	SF (C)	A	B	C	Cement	NS
M1 (F15)	0	-1	-1	15	0	0	84	1
M2 (F15G30)	0	1	-1	15	30	0	54	1
M3 (F15G30S6)	0	1	1	15	30	6	48	1
M4 (F15S6)	0	-1	1	15	0	6	78	1
M5 (S3)	-1	-1	0	0	0	3	96	1
M6 (G30S3)	-1	1	0	0	30	3	66	1
M7 (F30G30S3)	1	1	0	30	30	3	36	1
M8 (F30S3)	1	-1	0	30	0	3	66	1
M9 (F30G15S6)	1	0	1	30	15	6	48	1
M10 (F30G15)	1	0	-1	30	15	0	54	1
M11 (G15)	-1	0	-1	0	15	0	84	1
M12 (G15S6)	-1	0	1	0	15	6	78	1
M13 (F15G15S3)	0	0	0	15	15	3	66	1
M14 (F15G15S3)	0	0	0	15	15	3	66	1
M15 (F15G15S3)	0	0	0	15	15	3	66	1
M16 (only NS)	-	-	-	0	0	0	99	1
M17 (no NS)	-	-	-	0	0	0	100	0

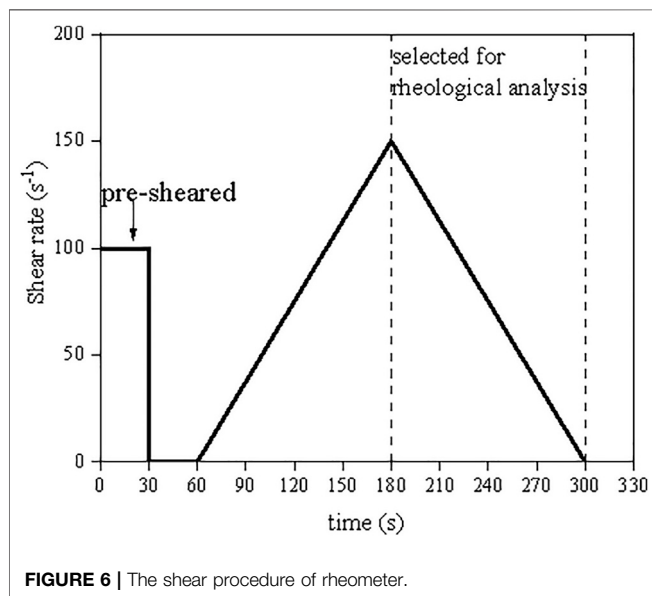


FIGURE 6 | The shear procedure of rheometer.

regression coefficients ($\beta_i, \beta_{ii}, \beta_{ij}$). R^2 was used to determine the degree of fitting of the quadratic term model to the data. At the same time, analysis of variance (ANOVA) was used to test the

significance of the variables. The flow chart of the research can be seen in **Figure 7**.

RESULTS AND DISCUSSION

Experimental and RSM Results

The experimental results of fluidity, yield stress, plastic viscosity, thixotropy, 3 d compressive strength (C_{3d}), 7 d compressive strength (C_{7d}), 28 d compressive strength (C_{28d}), and 56 d compressive strength (C_{56d}) are shown in **Table 4**, respectively. According to the data, ANOVA and quadratic term model fitting were carried on, respectively. The significance of variables and the regression coefficients ($\beta_i, \beta_{ii}, \beta_{ij}$) is shown in **Table 5**.

It can be seen from **Table 4** that compared with the group without NS (M17), the addition of NS (M16) remarkably decreased the fluidity and increased the yield stress, which can be due to the ultra-fine particle size led to the increase of friction and water demand (Chithra et al., 2016). Plastic viscosity and thixotropy are closely related to flocculation and C-S-H. NS has a higher pozzolanic effect, so the addition of NS accelerates the cement hydration to form additional C-S-H (Mendoza Reales et al., 2019). As a result, the plastic viscosity and thixotropy were

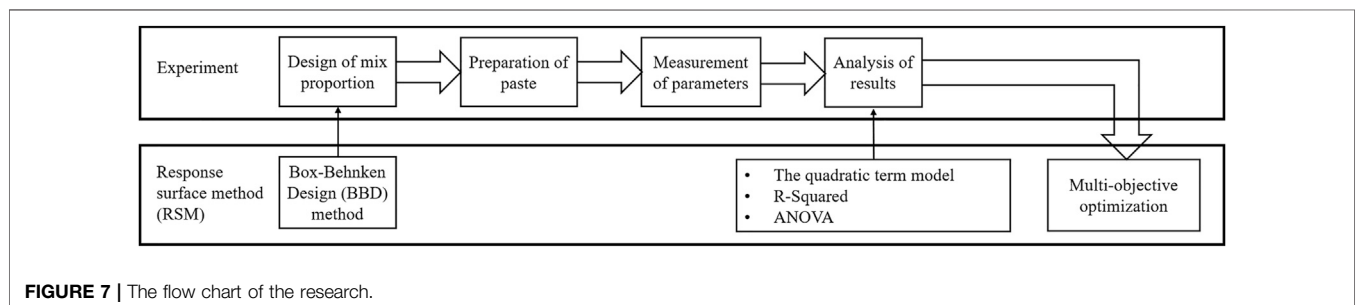


FIGURE 7 | The flow chart of the research.

TABLE 4 | Experimental results of nano-silica modified cement-based paste containing SCMs, fluidity.

Groups	Fluidity (mm)	Yield stress (Pa)	Plastic viscosity (Pa·s)	Thixotropy (Pa·s ⁻¹)	C _{3d} (MPa)	C _{7d} (MPa)	C _{28d} (MPa)	C _{56d} (MPa)
M1 (F15)	268	4.81	1.137	2,837	42.27	82.03	108.14	108.74
M2 (F15G30)	256	5.44	1.048	2,557	47.36	81.87	102.64	109.97
M3 (F15G30S6)	265	5.03	1.069	2,325	34.27	63.36	88.29	93.34
M4 (F15S6)	262	4.99	1.48	3,631	36.14	80.21	111.06	112.36
M5 (S3)	249	7.61	1.382	3,740	60.32	90.88	112.39	112.37
M6 (G30S3)	253	4.13	1.22	3,167	47.56	84.02	103.90	105.34
M7 (F30G30S3)	257	5.3	1.011	2,086	33.40	72.50	98.26	107.88
M8 (F30S3)	279	6.12	1.259	2,944	41.04	77.78	98.08	112.39
M9 (F30G15S6)	263	5.33	1.193	2,929	38.17	65.77	93.91	107.30
M10 (F30G15)	280	6.04	1.051	2,934	36.58	75.80	101.52	111.77
M11 (G15)	260	6.09	1.13	3,233	48.57	74.12	107.39	101.05
M12 (G15S6)	254	4.61	1.48	2,953	56.98	83.69	110.77	110.13
M13 (F15G15S3)	265	4.92	1.127	2,683	43.01	84.49	111.18	94.21
M14 (F15G15S3)	260	4.88	1.121	2,689	42.89	84.21	110.98	94.68
M15 (F15G15S3)	263	4.97	1.132	2,678	43.26	84.71	111.59	94.11
M16 (only NS)	253	5.17	1.445	4,629	59.38	98.05	110.77	108.87
M17 (no NS)	295	0.36	0.968	2,113	38.01	61.23	81.59	92.31

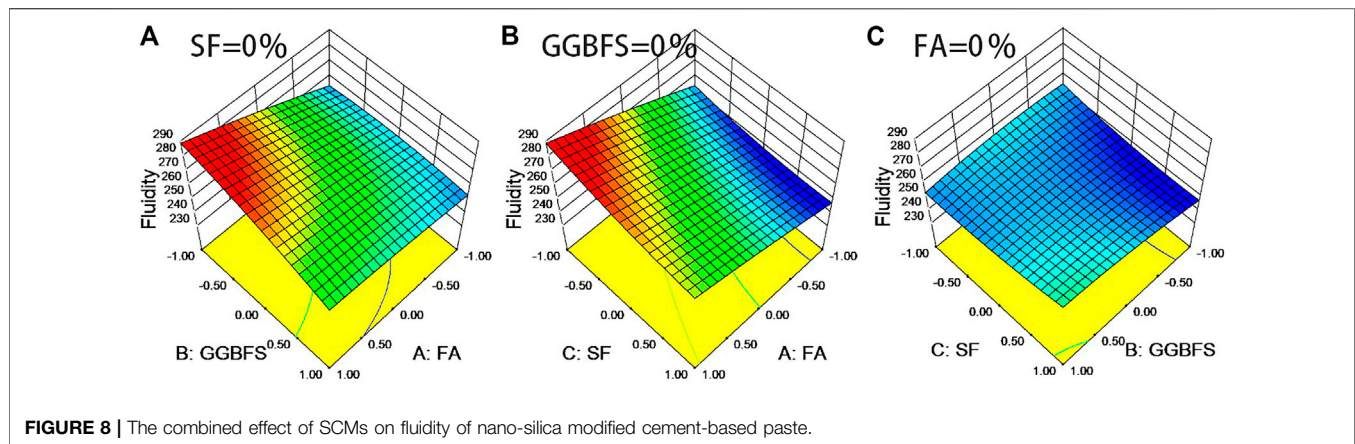
TABLE 5 | Results of ANOVA and regression coefficients.

Terms	Fluidity (mm)	Yield stress (Pa)	Plastic viscosity (Pa·s)	Thixotropy (Pa·s ⁻¹)	C _{3d} (MPa)	C _{7d} (MPa)	C _{28d} (MPa)	C _{56d} (MPa)	
Regression coefficients	Intercept	262.67	4.92	1.13	2,683.33	43.05	84.47	111.25	94.33
	A (x ₁)-FA	7.88*	0.04	-0.09***	-275.00*	-8.03*	-5.11**	-5.33**	1.30
	B (x ₂)-GGBFS	-3.38	-0.45	-0.11***	-377.13*	-2.15	-3.64*	-4.57*	-3.67*
	C (x ₃)-SF	-2.50	-0.30	0.11***	34.63	-1.15	-2.60	-1.96	-1.05
	AB (x ₁ x ₂)	-6.50*	0.67	-0.02	-71.25	1.28	0.39	2.17	0.63
	AC (x ₁ x ₃)	-2.75	0.19	-0.05**	68.75	-1.70	-4.90**	-2.75	-3.39
	BC (x ₂ x ₃)	3.75	-0.15	-0.08**	-256.50	-1.74	-4.17	-4.32	-5.06*
	A ² (x ₁ ²)	-0.83	0.66	0.06**	237.83	3.80	-2.60	-3.61	8.31**
	B ² (x ₂ ²)	-2.33	0.21	0.03	63.08	-1.27	-0.58	-4.48	6.85**
	C ² (x ₃ ²)	2.42	-0.06	0.03	91.08	-1.77	-7.03*	-4.24	4.92*
	R ²	0.9007	0.9213	0.9898	0.9851	0.9648	0.9635	0.9254	0.9401
	Adjusted R ²	0.8979	0.8934	0.9715	0.9218	0.9046	0.8935	0.8692	0.8323

increased in M16. Besides, the higher pozzolanic reactivity, nucleation effect, and filler effect also contributed to the increase of early strength through improving the microstructure (García-Taengua et al., 2015; Lu et al., 2020).

The regression coefficients obtained by fitting the quadratic term model can be seen in **Table 5** and the significance of the corresponding independent variable is also marked with * after the regression coefficient. If the *p*-value of the independent variable calculated through ANOVA is less than 0.001, it meant that it has an extremely significant effect on the corresponding parameters and marked with ***. **

represents highly significant *p* < 0.01 and * represents significant *p* < 0.05. Otherwise, the independent variable is not significant. Besides, the *R*² and the adjusted *R*² demonstrate the credibility of the quadratic term model. It can be seen from **Table 5** that the *R*² and the adjusted *R*² were both close to one demonstrating that the quadratic term model can be used to fit the data. In the next three sections, the quadratic term equation about every parameter was listed according to regression coefficients shown in **Table 5**. Moreover, response surface plots of the quadratic term model were also generated to understand the effect of the



independent variables on the dependent variable (WARDROP and MYERS, 1990; Garlapati and Roy, 2017).

Effect of SCMs on Fluidity

The relative influence of the independent variables can be evaluated by comparing their regression coefficients. The greater the absolute value, the greater the significance of the independent variable to the dependent variable. Besides, the positive value indicates that the factor can increase the parameter while the negative value demonstrates that the parameter decreases with increasing the factor. As can be seen from **Table 5** the effect of FA showed a significant positive effect on fluidity while the interaction of FA and GGBFS showed a significant negative effect. According to the regression coefficients, the quadratic term equation about fluidity can be written as follows and the combined effect of SCMs on fluidity is shown in **Figure 8**.

$$Y_{fluidity} = 262.67 + 7.88A - 3.38B - 2.5C - 0.83A^2 - 2.33B^2 + 2.42C^2 - 6.5AB - 2.75AC + 3.75BC. \quad (5)$$

It can be seen from **Eq. 5** that FA could increase the fluidity while the increase of GGBFS and SF led to the fluidity decrease. The effect of SCMs on fluidity can be ascribed to the morphology effect (Giergiczny, 2019). As can be seen from **Figure 2**, the spherical shape of FA can exhibit ball-bearing effect to decrease the friction between particles and increase the fluidity. However, GGBFS and SF have an irregular surface, which may increase the friction (Li and Wu, 2005; Jiao et al., 2017). Moreover, the specific surface area of SF is much larger than that of cement and the replacement of cement with SF can increase the demand for water to lubricating (Wu et al., 2019). As a result, the addition of GGBFS and SF decreased the fluidity. **Figure 8** shows the combined effect of SCMs on fluidity. **Figures 8A,B** illustrate that when the replacement of FA was 0% (that is FA = -1 level), the effect of GGBFS and SF on fluidity was not significant and the fluidity was kept at the range of 240–260 mm, which is consisted in **Figure 8C**. However, with the presence of FA, the addition of GGBFS and SF reduced the fluidity gradually and GGBFS reduced the most. This phenomenon is also reflected in

Table 5 in which FA*GGBFS showed a significant effect on fluidity compared with FA*SF. It also can be seen in **Figures 8A,B** that without SF and GGBFS, the incorporation of FA could increase the fluidity up to about 290 mm, which was comparable with the fluidity of M17 shown in **Table 4**. That indicated that the influence of FA and NS on fluidity could offset each other. Similar results are reported by other investigations (Shirdam et al., 2019; Xie et al., 2019). To increase fluidity, FA should be incorporated and the amount of GGBFS and SF should be as small as possible. At the same time, **Figure 8C** indicates that the combination of GGBFS and SF was not advisable.

Effect of SCMs on Rheology

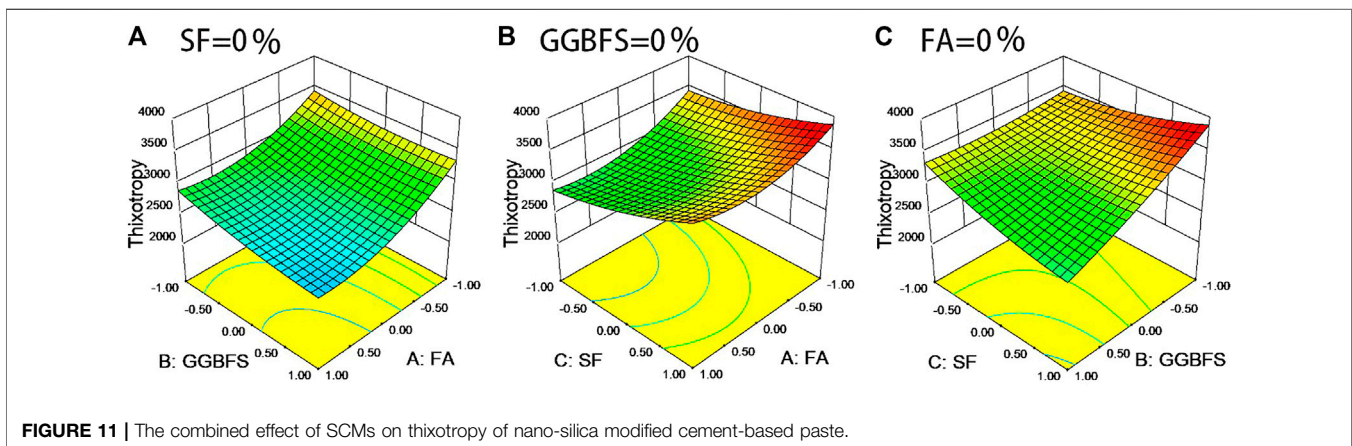
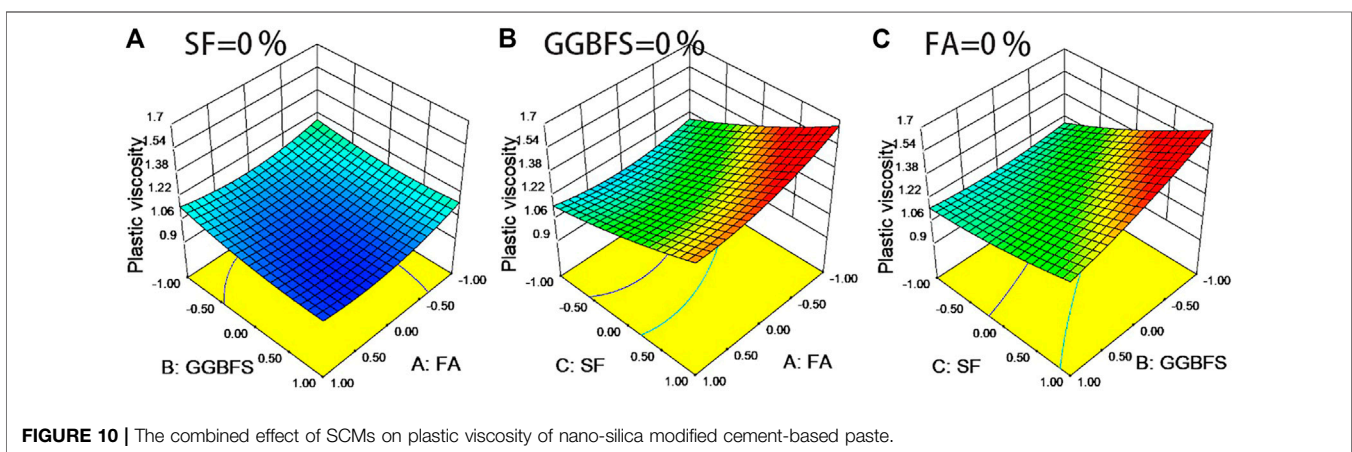
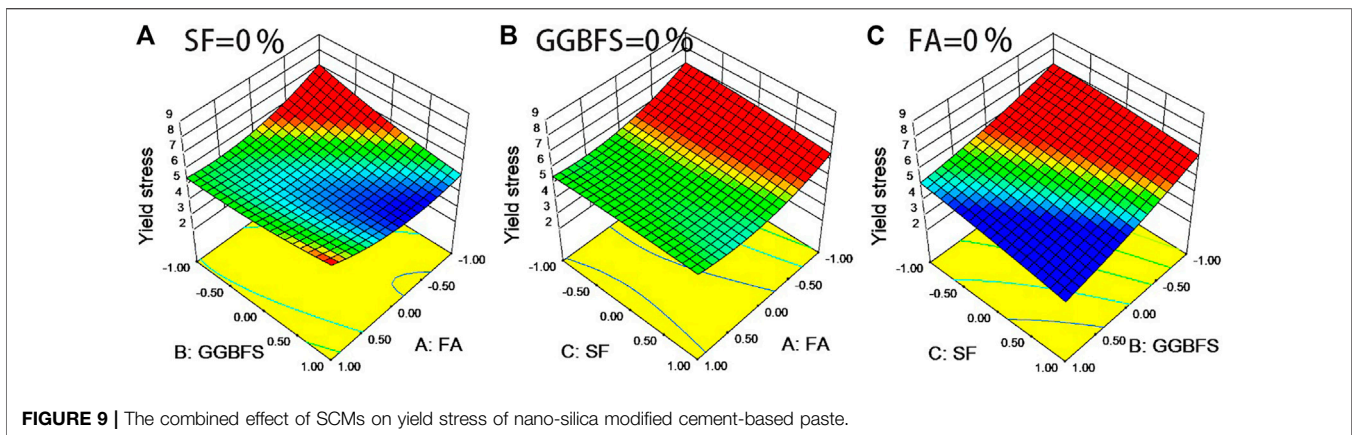
From **Table 5**, it also can be observed that the effect of SCMs on yield stress was not significant, but had a highly significant effect on plastic viscosity. Specifically, FA, GGBFS, and SF had an extremely significant effect and FA*SF and GGBFS*SF as well as FA² had a highly significant effect. Moreover, FA and GGBFS exhibited a negative effect on plastic viscosity while SF displayed a positive effect, which are consistent with Ref. (Ting et al., 2019; Duan et al., 2020; Jiang et al., 2020). As for thixotropy, FA, and GGBFS had a significant effect on thixotropy and the rest of the terms were not significant, the quadratic term model of the yield stress, plastic viscosity, and thixotropy are as follows:

$$Y_{yield\ stress} = 4.92 + 0.04A - 0.45B - 0.3C + 0.66A^2 + 0.21B^2 - 0.06C^2 + 0.67AB + 0.19AC - 0.15BC, \quad (6)$$

$$Y_{plastic\ viscosity} = 1.13 - 0.09A - 0.11B + 0.11C + 0.06A^2 + 0.03B^2 + 0.03C^2 - 0.02AB - 0.05AC - 0.08BC, \quad (7)$$

$$Y_{thixotropy} = 2683.33 - 275A - 377.13B + 34.63C + 237.83A^2 + 63.08B^2 + 91.08C^2 - 71.25AB + 68.75AC - 256.5BC. \quad (8)$$

The combined effect of SCMs on yield stress, plastic viscosity, and thixotropy is illustrated in **Figures 9–11**, respectively.



It can be seen from Eq. 6 that FA could increase the yield stress while GGBFS and SF made it decrease. However, Figure 9A shows that the incorporation of 30% FA (that is FA-1 level) made the yield stress increase slightly with GGBFS, which was not consistent with Eq. 6. At the same time, the incorporation of GGBFS made the lowest yield stress occurred at about FA-0 level, which indicated that there existed an interaction effect between

FA and GGBFS. Figure 9B illustrates that whether or not FA was added, the effect of SF on yield stress was not significant. On the contrary, the incorporation of FA decreased the yield stress sharply. That is in agreement with the result from Ref. (Shanahan et al., 2016). Banfill (Banfill, 1991) reported that the combination of GGBFS with SF resulted in lower yield stress, which is consistent with Figure 9C and Eq. 6. Based on

the discussion above, conclusions can be drawn that SF needs to be mixed with FA or GGBFS to reduce the yield stress. Among them, SF and GGBFS can exert a synergy effect to decrease the yield stress sharply. However, the amount of FA should be about 15% when mixed with GGBFS.

Equations 7, 8 show that both FA and GGBFS could decrease the plastic viscosity and thixotropy, but the addition of SF led to the two parameters' increase. From the perspective of microstructure, the plastic viscosity characterizes the deformation rate of the paste, which is mainly related to the amount of flocculated structure (Ke et al., 2020). Thixotropy can be explained by the formation and destruction of flocculated structures (Roussel et al., 2012). Moreover, the formation and amount of flocculated structure are related to the chemical reactivity of SCMs (Muzenda et al., 2020). The higher the chemical reactivity of SCMs, the more flocculated structure is generated and the less deformable the paste is, which leads to the higher plastic viscosity and thixotropy. Compared with cement, SF has higher chemical activity; as a result, the incorporation of SF leads to the formation of a large amount of flocculation rapidly (Benaicha et al., 2015). Jiao (Xiao et al., 2020) stated that GGBFS has lower hydraulic activity compared with cement, thus the addition of GGBFS decreases plastic viscosity. Moreover, the unburnt carbon coated on FA particles may decrease the chemical activity, thus decreasing the plastic viscosity and thixotropy (Alberici et al., 2017).

Figure 10A shows that the addition of FA and GGBFS decreased the plastic viscosity to about 0.9 Pa·s, which was comparable with the plastic viscosity of M17 shown in **Table 4**. On the contrary, SF increased the plastic viscosity up to about 1.7 Pa·s and adding FA or GGBFS may slightly decrease the plastic viscosity, which can be seen in **Figures 10B,C**. As for thixotropy, **Figures 11A,C** plot that the synergy effect of GGBFS and FA as well as GGBFS and SF could reduce thixotropy significantly. Among them, the addition of GGBFS changed the effect of SF on thixotropy, which indicated that SF was suitable for incorporation in the presence of GGBFS. However, the combination of FA and SF was not desirable because the lowest thixotropy was about 2,800 and occurred at FA-1 level and SF--1 level, which demonstrated that FA was not suitable for mixing with SF. Self-compacting concrete (SCC) often requires smaller plastic viscosity and thixotropy to obtain higher flow velocity (Alberici et al., 2017). From this point of view, the combinations of FA and GGBFS or SF and GGBFS are preferable while the combination of FA and SF is not advisable.

Effect of SCMs on Compressive Strength

Table 5 indicates that only FA had a significant effect on 3 d compressive strength. FA and FA*SF imposed a highly significant effect on 7 d compressive strength and followed by GGBFS and SF². Besides, GGBFS and FA exhibited significant and highly significant effects on 28 d compressive strength, respectively. Moreover, FA² and GGBFS² showed a highly significant effect on 56 d compressive strength and followed by GGBFS, GGBFS*SF, and SF². The fitted quadratic term equations of compressive strength are as follows:

$$Y_{3d\ C.S.} = 43.05 - 8.03A - 2.15B - 1.15C + 3.8A^2 - 1.27B^2 - 1.77C^2 + 1.28AB - 1.7AC - 1.74BC, \quad (9)$$

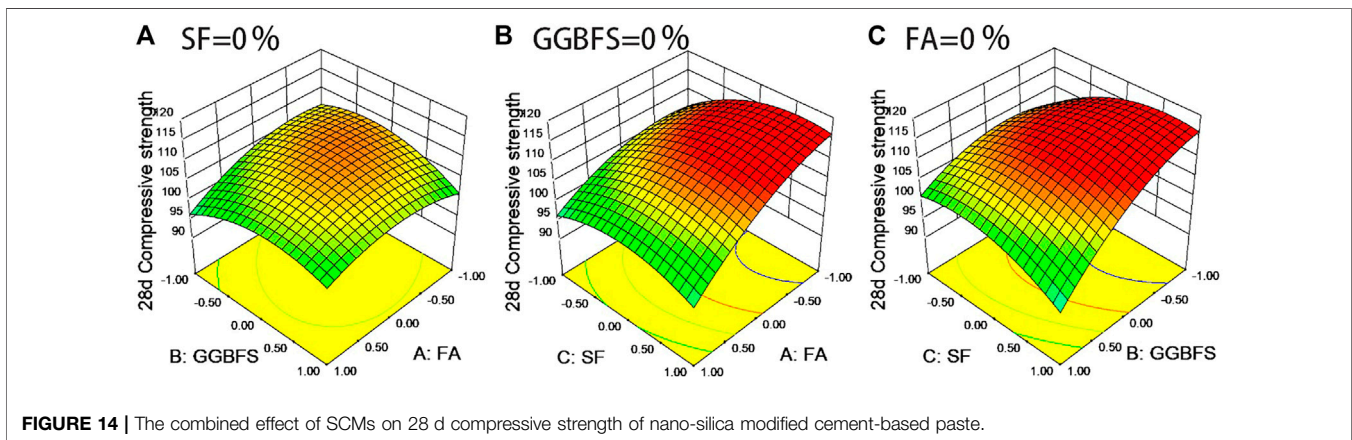
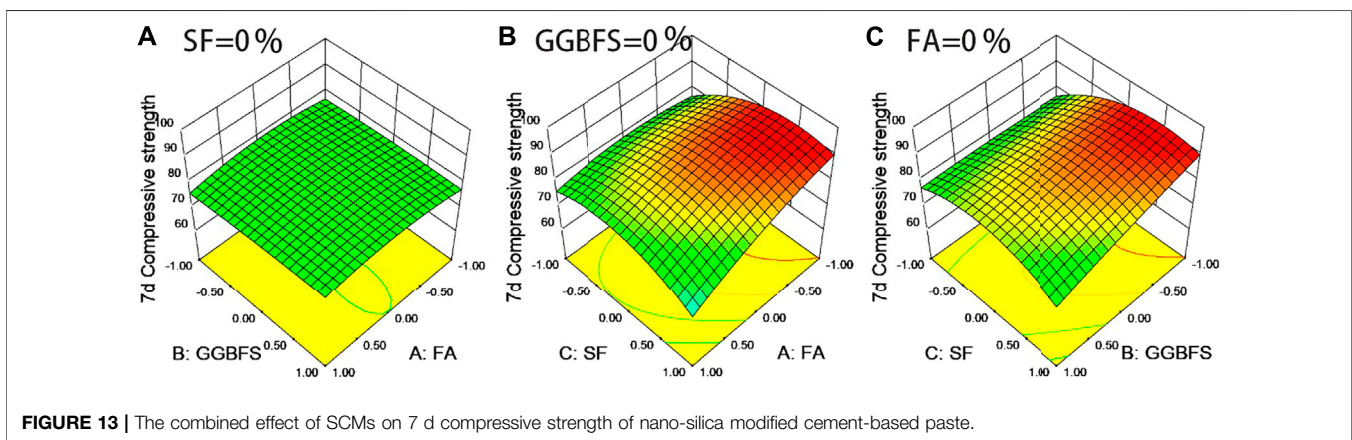
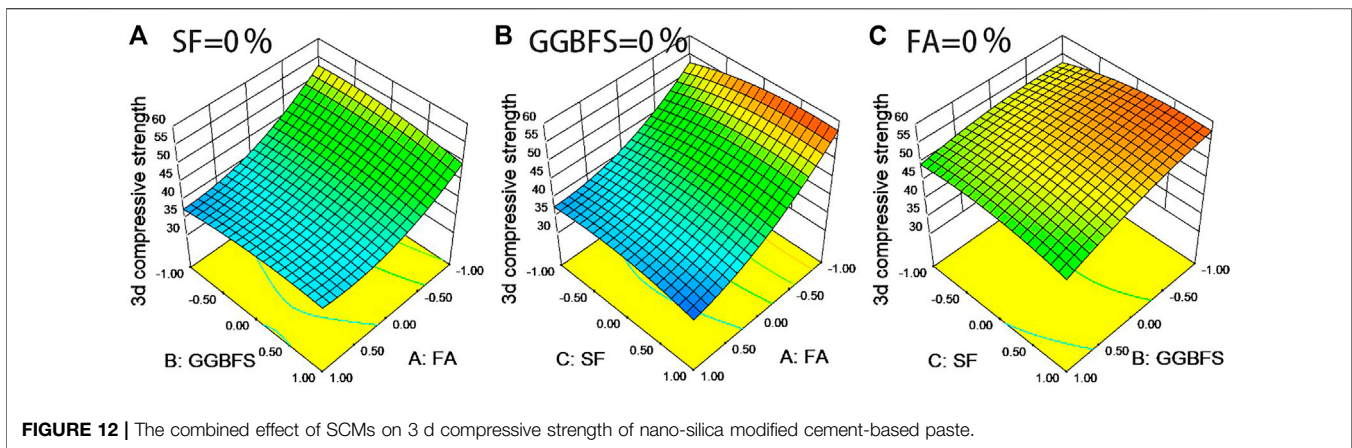
$$Y_{7d\ C.S.} = 84.47 - 5.11A - 3.64B - 2.6C - 2.6A^2 - 0.58B^2 - 7.03C^2 + 0.39AB - 4.9AC - 4.17BC, \quad (10)$$

$$Y_{28d\ C.S.} = 111.25 - 5.33A - 4.57B - 1.96C - 3.61A^2 - 4.48B^2 - 4.24C^2 + 2.17AB - 2.75AC - 4.32BC, \quad (11)$$

$$Y_{56d\ C.S.} = 94.33 + 1.3A - 3.67B - 1.05C + 8.31A^2 + 6.85B^2 + 4.92C^2 + 0.63AB - 3.39AC - 5.06BC. \quad (12)$$

It can be seen from **Eqs. 9–12** that SCMs can decrease the compressive strength, except FA which increased the 56 d compressive strength. This is because SCMs delay the early hydration and generate less C-S-H in an early age, which is closely related to compressive strength (Ting et al., 2020; Wang et al., 2020). The combined effect of SCMs on 3, 7, 28, and 56 d compressive strength is depicted in **Figures 12–15**, respectively. It can be seen from **Figures 12A,B** that the presence of FA decreased the 3 d compressive strength to about 36 MPa, which was similar to M17 shown in **Table 4**. However, the combination of SF and GGBFS kept the 3 d compressive strength at a higher level, which is shown in **Figure 12C**. **Figures 13, 14** indicate that SF played an important role to increase 7 and 28 d compressive strength. At the same time, in the presence of SF, the incorporation of FA or GGBFS would reduce the strength. Therefore, FA or GGBFS was not suitable to be incorporated into blends containing SF at a large amount. **Figure 14A** shows that the combination of GGBFS--0.5 level and FA--0.5 level contributed to the highest 28 d compressive strength while **Figure 15A** shows the same level to the lowest 56 d compressive strength, which indicated that the same combination of SCMs may have a different effect on compressive strength of different ages. Besides, in the presence of SF, the effect of FA and GGBFS on 56 d compressive strength was different. Specifically, the 56 d compressive strength decreased initially but then increased with the increase of FA while decreased steadily with the GGBFS. Moreover, it also can be seen from **Figures 13–15** that regardless of the amount of SCMs, the synergy effect of SCMs and NS increased the compressive strength compared with M17 shown in **Table 4**. Based on the above analysis, conclusions can be drawn that SF contributes to the compressive strength and GGBFS has a beneficial effect on 3 d strength. To obtain higher 7 and 28 d compressive strength, FA or GGBFS cannot be incorporated at a large amount in the presence of SF. As for 56 d compressive strength, the combination of FA and SF shows a satisfactory result compared with the other two combinations.

It can be seen from the above analysis that different SCMs have different effects on fluidity, rheology, and compressive strength of different ages. At the same time, the interaction between SCMs makes the effect more complicated. As a result, a more scientific



method should be utilized to optimize the mix proportion to achieve desirable properties.

MULTI-OBJECTIVE OPTIMIZATION

In this part, a multi-objective optimization technique was employed to find out the optimum solution (the appropriate

dosage of SCMs to satisfy target parameters). The criterion used to evaluate the response optimization is the desirability function. If one single response is needed to be optimized, then the individual desirability function should be used. Otherwise, the composite desirability function should be used. For example, if one wants to get maximum response, the desirability function is as follows (Ferdosian and Camões, 2017):

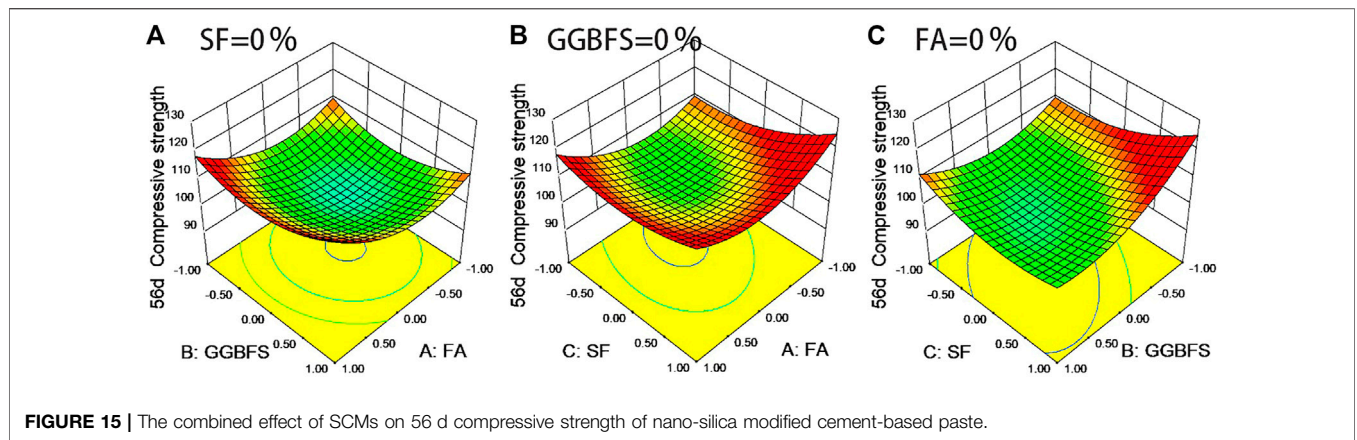


FIGURE 15 | The combined effect of SCMs on 56 d compressive strength of nano-silica modified cement-based paste.

TABLE 6 | The results of multi-objective optimization of nano-silica modified cement-based paste containing SCMs.

Coded values			Predicted values			Desirability
FA	GGBFS	SF	Fluidity (mm)	Plastic viscosity (Pa•s)	56 d compressive strength (MPa)	
0.96	-0.24	-0.97	280	1.08	112.39	0.947

$$d_i = \begin{cases} 0 & (Y_i < L_i) \\ \left[\frac{Y_i - L_i}{T_i - L_i} \right]^{w_i} & (L_i < Y_i < T_i), \\ 1 & (Y_i > T_i) \end{cases} \quad (13)$$

where d_i is the desirability; L_i is the lowest acceptable value of the i_{th} response; T_i is the highest acceptable value of the i_{th} response; w_i is the weight of the desirability function corresponding to the i_{th} response.

Besides, if the weight of the responses is equal, the composite desirability is calculated by

$$D = \sqrt[n]{d_1 \times d_2 \times \dots \times d_n}, \quad (14)$$

where n is the number of response.

Multi-objective optimization aims to find out the appropriate dosage of FA, GGBFS, and SF to satisfy the target parameters. Generally speaking, self-compacting concrete (SCC) needs the highest fluidity to satisfy its filling ability, the lowest plastic viscosity to provide higher flow velocity, and the highest compressive strength. In this part, taking the fluidity, plastic viscosity, and 56 d compressive strength as examples to perform multi-objective optimization and obtain the optimal proportion of SCMs, it should be noted that the primary objective is to obtain the maximum fluidity, minimum plastic viscosity, and maximum 56 d compressive strength. At the same time, the weights of the responses are supposed to be equal. The results of multi-objective optimization are shown in **Table 6**.

The dosage of SCMs corresponding to the coded value in **Table 6** can be calculated according to the linear relationship between the coded value and dosage in **Table 3**. It can be seen from **Table 6** that, to obtain the maximum fluidity, minimum plastic viscosity, and maximum 56 d compressive strength, the optimum additions of SF, FA, GGBFS, and SF were 29.4, 11.4, and

0.45%, respectively, and the desirability was 0.947. The abovementioned analysis showed that multi-objective optimization can be used to optimize the mix proportion.

CONCLUSION

In this study, the response surface method (RSM) was used to investigate the effect of SCMs on workability, rheology, and compressive strength of nano-silica modified cement-based paste. Box-Behnken design (BBD) method was used to design mix proportion and analysis of variance (ANOVA) was used to determine the significance of the factors. The quadratic term model was used for fitting the data and multi-objective optimization. Based on the results presented in this research, the following conclusions can be drawn:

- (1) FA could increase the fluidity and yield stress while GGBFS and SF made them decrease. FA should be incorporated in blends containing SF or GGBFS in order to obtain adequate fluidity. However, for the purpose of getting lower yield stress, SF needs to be mixed with FA or GGBFS and 15% of FA was advisable when mixed with GGBFS.
- (2) FA and GGBFS decreased the plastic viscosity and thixotropy, but SF led these two parameters to increase. Response surface plot indicated that, adding 30% GGBFS and 30% FA into nano-silica modified cement-based paste could decrease the plastic viscosity from 1.445 to 0.9 Pa•s, which was similar with reference sample (M17). Thus, SCMs could improve the rheology of nano-silica modified cement-based paste. In terms of quaternary blends, the combinations of FA and GGBFS or SF and GGBFS were preferable to achieve lower plastic viscosity and thixotropy.

- (3) Regardless of the amount of SCMs, the synergy effect of SCMs and NS increased the 7, 28, and 56 d compressive strength higher than that of reference sample (M17). The amount of FA and GGBFS should be less than 15% when mixed with SF in order to obtain higher 7 and 28 d compressive strength. As for 56 d compressive strength, the combination of FA and SF was acceptable compared with other two combinations.
- (4) The optimal mix proportion of SCMs was difficult to calculate to obtain satisfied parameters due to the interaction between SCMs. Therefore, multi-objective optimization can be successfully applied to optimize the mix proportion to achieve desirable target.

DATA AVAILABILITY STATEMENT

The raw data supporting the conclusions of this article will be made available by the authors, without undue reservation.

REFERENCES

- Ahmed, T. W., Ali, A. A. M., and Zidan, R. S. (2020). Properties of High Strength Polypropylene Fiber concrete Containing Recycled Aggregate. *Construction Building Mater.* 241, 118010. doi:10.1016/j.conbuildmat.2020.118010
- Alberici, S., Beer, J. d., Hoorn, I. v. d., and Maarten, S. (2017). *Fly Ash and Blast Furnace Slag for Cement Manufacturing*. BEIS Research. Paper No. 19.
- Banfill, P. F. G. (1991). Rheology of Fresh Cement and Concrete. *Rheology Reviewers*, J537, 61–130. Rheology of fresh cement and concrete. doi:10.4324/9780203473290
- Benaicha, M., Roguiez, X., Jalbaud, O., Burtschell, Y., and Alaoui, A. H. (2015). Influence of Silica Fume and Viscosity Modifying Agent on the Mechanical and Rheological Behavior of Self Compacting concrete. *Construction Building Mater.* 84, 103–110. doi:10.1016/j.conbuildmat.2015.03.061
- Cheng, S., Shui, Z., Sun, T., Yu, R., and Zhang, G. (2018). Durability and Microstructure of Coral Sand concrete Incorporating Supplementary Cementitious Materials. *Construction Building Mater.* 171, 44–53. doi:10.1016/j.conbuildmat.2018.03.082
- Chithra, S., Senthil Kumar, S. R. R., and Chinnaraju, K. (2016). The Effect of Colloidal Nano-Silica on Workability, Mechanical and Durability Properties of High Performance Concrete with Copper Slag as Partial fine Aggregate. *Construction Building Mater.* 113, 794–804. doi:10.1016/j.conbuildmat.2016.03.119
- Committee, C. N. S. M. (2016). *Common Portland Cement (GB175-2007*. Beijing: Chinese Standard Publishing.
- de Larrard, F., Ferraris, C. F., and Sedran, T. (1998). Fresh concrete: A Herschel-Bulkley Material. *Mat. Struct.* 31, 494–498. Fresh concrete. doi:10.1007/bf02480474
- Dhanya, B. S., Santhanam, M., Gettu, R., and Pillai, R. G. (2018). Performance Evaluation of Concretes Having Different Supplementary Cementitious Material Dosages Belonging to Different Strength Ranges. *Construction Building Mater.* 187, 984–995. doi:10.1016/j.conbuildmat.2018.07.185
- Duan, Z., Hou, S., Xiao, J., and Singh, A. (2020). Rheological Properties of Mortar Containing Recycled Powders from Construction and Demolition Wastes. *Construction Building Mater.* 237, 117622. doi:10.1016/j.conbuildmat.2019.117622
- Ferdosian, I., and Camões, A. (2017). Eco-efficient Ultra-high Performance concrete Development by Means of Response Surface Methodology. *Cement and Concrete Composites* 84, 146–156. doi:10.1016/j.cemconcomp.2017.08.019
- Ferron, R., Gregori, A., Sun, Z., and Shah, S. P. (2007). Rheological Method to Evaluate Structural Buildup in Self-Consolidating concrete Cement Pastes. *ACI MATERIALS JOURNAL* 107, 104. doi:10.1088/0957-4484/18/17/17560110.14359/18669
- Flores, Y. C., Cordeiro, G. C., Toledo Filho, R. D., and Tavares, L. M. (2017). Performance of Portland Cement Pastes Containing Nano-Silica and Different
- Types of Silica. *Construction Building Mater.* 146, 524–530. doi:10.1016/j.conbuildmat.2017.04.069
- García-Taengua, E., Sonebi, M., Hossain, K. M. A., Lachemi, M., and Khatib, J. (2015). Effects of the Addition of Nanosilica on the Rheology, Hydration and Development of the Compressive Strength of Cement Mortars. *Composites B: Eng.* 81, 120–129. doi:10.1016/j.compositesb.2015.07.009
- Garlapati, V. K., and Roy, L. (2017). Utilization of Response Surface Methodology for Modeling and Optimization of Tablet Compression Process. *Jyp* 9 (3), 417–421. doi:10.5530/jyp.2017.9.82
- Ghafari, E., Costa, H., Júlio, E., Portugal, A., and Durães, L. (2014). The Effect of Nanosilica Addition on Flowability, Strength and Transport Properties of Ultra High Performance concrete. *Mater. Des.* 59, 1–9. doi:10.1016/j.matdes.2014.02.051
- Ghalehnovi, M., Rashki, M., and Ameryan, A. (2020). First Order Control Variates Algorithm for Reliability Analysis of Engineering Structures. *Appl. Math. Model.* 77, 829–847. doi:10.1016/j.apm.2019.07.049
- Giergiczny, Z. (2019). Fly Ash and Slag. *Cement Concrete Res.* 124, 105826. doi:10.1016/j.cemconres.2019.105826
- Hosan, A., and Shaikh, F. U. A. (2021). Influence of Nano Silica on Compressive Strength, Durability, and Microstructure of High-volume Slag and High-volume Slag-Fly Ash Blended Concretes. *Struct. Concrete* 22, E474–E487. doi:10.1002/suco.202000251
- Hou, P., Wang, K., Qian, J., Kawashima, S., Kong, D., and Shah, S. P. (2012). Effects of Colloidal nanoSiO₂ on Fly Ash Hydration. *Cement and Concrete Composites* 34 (10), 1095–1103. doi:10.1016/j.cemconcomp.2012.06.013
- Hou, P., Kawashima, S., Kong, D., Corr, D. J., Qian, J., and Shah, S. P. (2013). Modification Effects of Colloidal nanoSiO₂ on Cement Hydration and its Gel Property. *Composites Part B: Eng.* 45 (1), 440–448. doi:10.1016/j.compositesb.2012.05.056
- Hu, C., and de Larrard, F. (1996). The Rheology of Fresh High-Performance Concrete. *Cement Concrete Res.* 26, 283–294. doi:10.1016/0008-8846(95)00213-8
- ASTM International (2014). *ASTM C230/C230M-20, Standard Specification for Flow Table for Use in Tests of Hydraulic Cement*.
- Jalal, M., Teimortashlu, E., and Grasley, Z. (2019). Performance-based Design and Optimization of Rheological and Strength Properties of Self-Compacting Cement Composite Incorporating Micro/Nano Admixtures. *Composites Part B: Eng.* 163, 497–510. doi:10.1016/j.compositesb.2019.01.028
- Jiang, D., Li, X., Lv, Y., Zhou, M., He, C., Jiang, W., et al. (2020). Utilization of limestone Powder and Fly Ash in Blended Cement: Rheology, Strength and Hydration Characteristics. *Construction Building Mater.* 232, 117228. doi:10.1016/j.conbuildmat.2019.117228
- Jiao, D., Shi, C., Yuan, Q., An, X., Liu, Y., and Li, H. (2017). Effect of Constituents on Rheological Properties of Fresh concrete-A Review. *Cement and Concrete Composites* 83, 146–159. doi:10.1016/j.cemconcomp.2017.07.016

AUTHOR CONTRIBUTIONS

All authors listed have made a substantial, direct, and intellectual contribution to the work and approved it for publication.

FUNDING

The authors gratefully acknowledge financial supports from the National Natural Science Foundation of China (Grant No. 51778269), National Key Research and Development Program of China (Grant No. 2017YFC0703100), and Case-by-Case Project for Top Outstanding Talents of Jinan.

ACKNOWLEDGMENTS

The authors thank Tafadzwa Ronald Muzenda for his help in proofreading.

- Jiao, D., Shi, C., Yuan, Q., An, X., and Liu, Y. (2018). Mixture Design of concrete Using Simplex Centroid Design Method. *Cement and Concrete Composites* 89, 76–88. doi:10.1016/j.cemconcomp.2018.03.001
- Nandhini, K., and Ponmalar, V. (2018). Microstructural Behaviour and Flowing Ability of Self-compacting concrete Using Micro- and Nano-silica. *Micro Nano Lett.* 13 (8), 1213–1218. doi:10.1049/mnl.2018.0105
- Kawashima, S., Chauuche, M., Corr, D. J., and Shah, S. P. (2013). Rate of Thixotropic Rebuilding of Cement Pastes Modified with Highly Purified Attapulgite Clays. *Cement Concrete Res.* 53, 112–118. doi:10.1016/j.cemconres.2013.05.019
- Ke, G., Zhang, J., Xie, S., and Pei, T. (2020). Rheological Behavior of Calcium Sulfoaluminate Cement Paste with Supplementary Cementitious Materials. *Construction Building Mater.* 243, 118234. doi:10.1016/j.conbuildmat.2020.118234
- Kong, D., Du, X., Wei, S., Zhang, H., Yang, Y., and Shah, S. P. (2012). Influence of Nano-Silica Agglomeration on Microstructure and Properties of the Hardened Cement-Based Materials. *Construction Building Mater.* 37, 707–715. doi:10.1016/j.conbuildmat.2012.08.006
- Li, G., and Wu, X. (2005). Influence of Fly Ash and its Mean Particle Size on Certain Engineering Properties of Cement Composite Mortars. *Cement Concrete Res.* 35 (6), 1128–1134. doi:10.1016/j.cemconres.2004.08.014
- Li, N., Shi, C., Zhang, Z., Zhu, D., Hwang, H.-J., Zhu, Y., et al. (2018). A Mixture Proportioning Method for the Development of Performance-Based Alkali-Activated Slag-Based concrete. *Cement and Concrete Composites* 93, 163–174. doi:10.1016/j.cemconcomp.2018.07.009
- Liu, M., Tan, H., and He, X. (2019). Effects of Nano-SiO₂ on Early Strength and Microstructure of Steam-Cured High Volume Fly Ash Cement System. *Construction Building Mater.* 194, 350–359. doi:10.1016/j.conbuildmat.2018.10.214
- Lu, J., Jiang, J., Lu, Z., Li, J., Niu, Y., and Yang, Y. (2020). Pore Structure and Hardened Properties of Aerogel/cement Composites Based on Nanosilica and Surface Modification. *Construction Building Mater.* 245, 118434. doi:10.1016/j.conbuildmat.2020.118434
- Mendoza Reales, O. A., Duda, P., Silva, E. C. C. M., Paiva, M. D. M., and Filho, R. D. T. (2019). Nanosilica Particles as Structural Buildup Agents for 3D Printing with Portland Cement Pastes. *Construction Building Mater.* 219, 91–100. doi:10.1016/j.conbuildmat.2019.05.174
- Muzenda, T. R., Hou, P., Kawashima, S., Sui, T., and Cheng, X. (2020). The Role of limestone and Calcined clay on the Rheological Properties of LC3. *Cement and Concrete Composites* 107, 103516. doi:10.1016/j.cemconcomp.2020.103516
- Park, C. K., Noh, M. H., and Park, T. H. (2005). Rheological Properties of Cementitious Materials Containing mineral Admixtures. *Cement Concrete Res.* 35 (5), 842–849. doi:10.1016/j.cemconres.2004.11.002
- Pizoń, J., Miera, P., and Łaźniewska-Piekarczyk, B. (2016). Influence of Hardening Accelerating Admixtures on Properties of Cement with Ground Granulated Blast Furnace Slag. *Proced. Eng.* 161, 1070–1075. doi:10.1016/j.proeng.2016.08.850
- Pizoń, J. (2017). Long-term Compressive Strength of Mortars Modified with Hardening Accelerating Admixtures. *Proced. Eng.* 195, 205–211. doi:10.1016/j.proeng.2017.04.545
- Pratama, H. B., Supijo, M. C., and Sutopo, H. B. (2020). Experimental Design and Response Surface Method in Geothermal Energy: A Comprehensive Study in Probabilistic Resource Assessment. *Geothermics* 87, 101869. doi:10.1016/j.geothermics.2020.101869
- Qian, Y., Lesage, K., El Cheikh, K., and De Schutter, G. (2018). Effect of Polycarboxylate Ether Superplasticizer (PCE) on Dynamic Yield Stress, Thixotropy and Flocculation State of Fresh Cement Pastes in Consideration of the Critical Micelle Concentration (CMC). *Cement Concrete Res.* 107, 75–84. doi:10.1016/j.cemconres.2018.02.019
- Ramezani-pour, A. A., and Moieni, M. A. (2018). Mechanical and Durability Properties of Alkali Activated Slag Coating Mortars Containing Nanosilica and Silica Fume. *Construction Building Mater.* 163, 611–621. doi:10.1016/j.conbuildmat.2017.12.062
- Riding, K., Silva, D. A., and Scrivener, K. (2010). Early Age Strength Enhancement of Blended Cement Systems by CaCl₂ and Diethanol-Isopropanolamine. *Cement Concrete Res.* 40 (6), 935–946. doi:10.1016/j.cemconres.2010.01.008
- Roshani, A., and Fall, M. (2020). Flow Ability of Cemented Pastefill Material that Contains Nano-Silica Particles. *Powder Tech.* 373, 289–300. doi:10.1016/j.powtec.2020.06.050
- Roussel, N., Ovarlez, G., Garrault, S., and Brumaud, C. (2012). The Origins of Thixotropy of Fresh Cement Pastes. *Cement Concrete Res.* 42 (1), 148–157. doi:10.1016/j.cemconres.2011.09.004
- Roussel, N. (2006). A Thixotropy Model for Fresh Fluid Concretes: Theory, Validation and Applications. *Cement Concrete Res.* 36 (10), 1797–1806. doi:10.1016/j.cemconres.2006.05.025
- Senff, L., Labrincha, J. A., Ferreira, V. M., Hotza, D., and Repette, W. L. (2009). Effect of Nano-Silica on Rheology and Fresh Properties of Cement Pastes and Mortars. *Construction Building Mater.* 23 (7), 2487–2491. doi:10.1016/j.conbuildmat.2009.02.005
- Shanahan, N., Tran, V., Williams, A., and Zayed, A. (2016). Effect of SCM Combinations on Paste Rheology and its Relationship to Particle Characteristics of the Mixture. *Construction Building Mater.* 123, 745–753. doi:10.1016/j.conbuildmat.2016.07.094
- Shirdam, R., Amini, M., and Bakhshi, N. (2019). Investigating the Effects of Copper Slag and Silica Fume on Durability, Strength, and Workability of Concrete. *Int. J. Environ. Res.* 13 (6), 909–924. doi:10.1007/s41742-019-00215-7
- Supervision, N. B. o. Q. a. T. (1999). *GB/T 17671-1999, Method of Testing Cements-Determination of Strength.*
- Ting, L., Qiang, W., and Shiyu, Z. (2019). Effects of Ultra-fine Ground Granulated Blast-Furnace Slag on Initial Setting Time, Fluidity and Rheological Properties of Cement Pastes. *Powder Tech.* 345, 54–63. doi:10.1016/j.powtec.2018.12.094
- Ting, L., Qiang, W., and Yuqi, Z. (2020). Influence of Ultra-fine Slag and Silica Fume on Properties of High-Strength concrete. *Mag. Concrete Res.* 72 (12), 610–621. doi:10.1680/jmacr.18.00492
- Wang, X., Huang, J., Ma, B., Dai, S., Jiang, Q., and Tan, H. (2019). Effect of Mixing Sequence of Calcium Ion and Polycarboxylate Superplasticizer on Dispersion of a Low Grade Silica Fume in Cement-Based Materials. *Construction Building Mater.* 195, 537–546. doi:10.1016/j.conbuildmat.2018.11.032
- Wang, L., Guo, F., Lin, Y., Yang, H., and Tang, S. W. (2020). Comparison between the Effects of Phosphorous Slag and Fly Ash on the C-S-H Structure, Long-Term Hydration Heat and Volume Deformation of Cement-Based Materials. *Construction Building Mater.* 250, 118807. doi:10.1016/j.conbuildmat.2020.118807
- Wardrop, D. M., and Myers, R. H. (1990). Some Response Surface Designs for Finding Optimal Conditions. *J. Stat. Plann. inference* 25 (1), 7–28. doi:10.1016/0378-3758(90)90003-D
- Wu, Z., Khayat, K. H., and Shi, C. (2019). Changes in Rheology and Mechanical Properties of Ultra-high Performance concrete with Silica Fume Content. *Cement Concrete Res.* 123, 105786. doi:10.1016/j.cemconres.2019.105786
- Xiao, Y., Ye, K., and He, W. (2020). An Improved Response Surface Method for Fragility Analysis of Base-Isolated Structures Considering the Correlation of Seismic Demands on Structural Components. *Bull. Earthquake Eng.* 18, 4039–4059. doi:10.1007/s10518-020-00836-w
- Xie, J., WangRao, J. R., Rao, R., Wang, C., and Fang, C. (2019). Effects of Combined Usage of GGBS and Fly Ash on Workability and Mechanical Properties of Alkali Activated Geopolymer concrete with Recycled Aggregate. *Composites Part B: Eng.* 164, 179–190. doi:10.1016/j.compositesb.2018.11.067
- Xiuzhi, Z., Hailong, S., Haibo, Y., Ru, M., and Heng, C. (2021). Rheological Properties of Nanosilica-Modified Cement Paste at Different Temperatures and Hydration Times. *J. Mater. Civil Eng.* 33 (1), 402040. doi:10.1061/(ASCE)MT.1943-5533.0003488
- Yan-Rong, Z., Xiang-Ming, K., Zi-Chen, L., Zhen-Bao, L., Qing, Z., Bi-Qin, D., et al. (2016). Influence of Triethanolamine on the Hydration Product of Portlandite in Cement Paste and the Mechanism. *Cement Concrete Res.* 87, 64–76. doi:10.1016/j.cemconres.2016.05.009

Conflict of Interest: The authors declare that the research was conducted in the absence of any commercial or financial relationships that could be construed as a potential conflict of interest.

Publisher's Note: All claims expressed in this article are solely those of the authors and do not necessarily represent those of their affiliated organizations, or those of the publisher, the editors, and the reviewers. Any product that may be evaluated in this article, or claim that may be made by its manufacturer, is not guaranteed or endorsed by the publisher.

Copyright © 2021 Zhang, Lin, Bi, Sun, Chen, Li and Mu. This is an open-access article distributed under the terms of the Creative Commons Attribution License (CC BY). The use, distribution or reproduction in other forums is permitted, provided the original author(s) and the copyright owner(s) are credited and that the original publication in this journal is cited, in accordance with accepted academic practice. No use, distribution or reproduction is permitted which does not comply with these terms.